

# Non-quantum liquefaction of coherent gases

David Novoa, Humberto Michinel, Daniele Tommasini and María I. Rodas-Verde  
*Departamento de Física Aplicada, Facultade de Ciencias de Ourense,  
Universidade de Vigo, As Lagoas s/n, Ourense, ES-32004 Spain.*

We show that a gas-to-liquid phase transition at zero temperature may occur in a coherent gas of bosons in the presence of competing nonlinear effects. This situation can take place both in atomic systems like Bose-Einstein Condensates in alkali gases with two and three-body interactions of opposite signs, as well as in laser beams which propagate through optical media with Kerr (focusing) and higher order (defocusing) nonlinear responses. The liquefaction process takes place in absence of any quantum effect and can be formulated in the frame of a mean field theory, in terms of the minimization of a thermodynamic potential. We also show numerically that the effect of linear gain and three-body recombination also provides a rich dynamics with the emergence of self-organization behaviour.

PACS numbers: 03.75.Lm, 42.65.Jx, 42.65.Tg

Keywords: phase-transition, liquefaction, solitons, filamentation, cold atoms

## I. INTRODUCTION

Paraxial propagation of linearly polarized laser beams through transparent optical media with intensity dependent refractive index is mathematically equivalent to the free evolution of the wavefunction order parameter used in the mean-field description of a two-dimensional gas of  $N$  interacting atoms in a Bose-Einstein Condensate (BEC) at temperature  $T = 0K$  [1]. Both systems can be modeled by identical nonlinear Schrödinger equations[2]. For photons in the laser beam, the  $\chi^{(n)}$  component of the nonlinear optical susceptibility plays the same role as  $n$ -body interactions between atoms in the cloud and the propagation constant can be identified with a chemical potential for the light distribution. As all the photons in a coherent wave are equal, the laser beam can be treated on equal foot as any system of  $N$  identical interacting bosons at zero temperature[3].

The previous point of view, which takes into account the equivalence between laser beams and BECs of ultracold atoms, has led to an interesting suggestion made by Chiao[4], who recently proposed to verify the superfluidity of coherent light, in analogy with degenerate quantum atomic gases. More recently, similar concepts have been successfully used to analyze condensation phenomena of nonlinear waves[5] and quantum phase transitions of photons in periodic lattices[6].

In Chiao's model the key point of the analysis is "*same equations, same predictions*" and therefore photons from a monochromatic laser source are considered as an ideal bosonic gas at zero temperature in which continuous phase transitions (CPT) can take place due to long range quantum fluctuations around the ground state[7]. These critical phenomena are thus called *quantum* phase transitions (QPT)[8] to distinguish them from the standard phase changes which are well-known in classical thermodynamics.

As we will show in this work, CPT may occur in any *classical* system at zero temperature without long range quantum correlations involved, if opposite nonlinear in-

teractions are present. In the case of Chiao's "superfluid light" the phase transition is produced by effect of a defocusing intensity-dependent refractive index[9] and thus a waveguide is used to avoid spreading of the beam (in the same way as magneto-optical traps are employed to hold atomic BECs). However, as superfluidity may occur both in gases and liquids, it cannot be considered as a trace of the presence of a liquid state[10, 11]; it is also required the appearance of surface tension effects[12]. Moreover, in Chiao's model, the interactions between particles are repulsive and they cannot drive a gas-liquid transition.

Thus, in this work we will follow the same lines of thought to suggest the possibility of obtaining a gas-to-liquid phase transition in a classical gas at  $T = 0K$  described in a mean field theory by the so-called *cubic-quintic* (CQ) model with competing nonlinearities. Several pioneering works have highlighted the interesting properties of this CQ-model[13]. Cavitation, superfluidity and coalescence have been investigated[14, 15] in the context of liquid He, where the model is a simple approach if nonlocal interactions are not taken into account. Stable optical vortex solitons and the existence of top-flat states have been also reported in optical materials with CQ optical susceptibility[16, 17]. The surface tension properties that appear in this system[18] have been considered as a trace of a "liquid state of light"[10].

On the other hand, recent experiments about filamentation of high-power laser pulses in  $CS_2$  have shown that the CQ nonlinearity is achievable in this material[19]. It has been also suggested that atomic coherence may be used to induce a giant CQ-like refractive index of a Rb gas[11]. Thus, the practical realization of the first "liquid of light" state as an example of non-quantum liquefaction at zero temperature is close. In BEC systems, a CQ-model can be used in the mean field description of an ultracold gas at zero temperature in the presence of Efimov states with tunable two- and three-body interactions, which have been recently proposed[20].

## II. MATHEMATICAL ANALYSIS

The cubic-quintic model describes a coherent bosonic system of  $N$  particles with two- and three-body interactions. The mathematical formulation of the mean field theory yields a generalised non-linear Schrödinger (NLS, also called Gross-Pitaevskii) equation of the form:

$$i\frac{\partial\Psi}{\partial\eta} + \frac{1}{2}\nabla_{\perp}^2\Psi + \gamma|\Psi|^2\Psi - \delta|\Psi|^4\Psi = 0, \quad (1)$$

If the system modeled by the previous equation is a photon gas, the above NLS describes paraxial propagation of a continuous linearly-polarized laser beam of wavelength  $\lambda$  in a nonlinear medium with a refractive index depending on the intensity  $I$  in the form  $n = n_0 + n_2I - n_4I^2$  and the adimensional variables are:  $\eta$  the propagation distance multiplied by  $2\pi/\lambda$ ,  $|\Psi|^2$  the beam irradiance multiplied by the Kerr coefficient  $n_2 = \gamma$ ,  $n_4 = \delta$  an adimensional parameter indicating the strength of the quintic nonlinear optical susceptibility, and  $\nabla_{\perp}^2 = \partial^2/\partial x^2 + \partial^2/\partial y^2$  the transverse Laplacian operator, where  $x$  and  $y$  are the transverse spatial dimensions multiplied by  $2\pi\sqrt{2n_0}/\lambda$ .

In the case of a two-dimensional atomic BEC tightly trapped along one axis by a parabolic potential of frequency  $\nu_{\perp}$  and thickness  $r_{\perp} = \sqrt{\hbar/m\nu_{\perp}}$ , the adimensional variables correspond to:  $\eta$  the time in units of  $\nu_{\perp}^{-1}$ ,  $|\Psi|^2$  the atomic density multiplied by two-body coefficient  $\gamma$ ,  $\delta$  an adimensional parameter indicating the strength of the three-body interactions, and  $\nabla_{\perp}^2 = \partial^2/\partial x^2 + \partial^2/\partial y^2$  the transverse Laplacian operator, where  $x$  and  $y$  are the transverse spatial dimensions divided by  $r_{\perp}$ .

Recent experiments for beam propagation in  $CS_2$ [19] at  $\lambda = 800nm$  yield the following values for the above parameters in the case of laser beams:  $n_0 = 1.6$ ,  $n_2 = 3 \cdot 10^{-15}cm^2/W$  and  $n_4 = 2 \cdot 10^{-27}cm^4/W^2$ . Other materials like air[21] or chalcogenide glasses[22] seem to display the C-Q behavior usually accompanied by ionization and non-linear losses. It has been also pointed the possibility of engineering this type of optical response by quantum techniques which allow to access this nonlinear regime with milliwatt ultrastabilized lasers[11]. For atomic BEC systems it has been proposed that a combination of two-body (attractive) and three-body (repulsive) elastic interactions can yield liquid *boselets*[24]. This behaviour can be explained in terms of the Efimov states[20]. However, three-body scattering in BECs has inelastic contributions and yields highly nonlinear losses. This means that in the most general case the coefficient  $\delta$  in equation (1) may be complex both for laser systems as well as for atomic gases.

The above CQ-NLSE admits soliton-like solutions of finite size[13] of the form  $\Psi_A(x, y, \eta) = A(x, y)e^{-i\mu\eta}$ , being  $\mu$  the propagation constant in the case of light and the chemical potential for atomic BECs. These solitons can only be calculated numerically and coex-

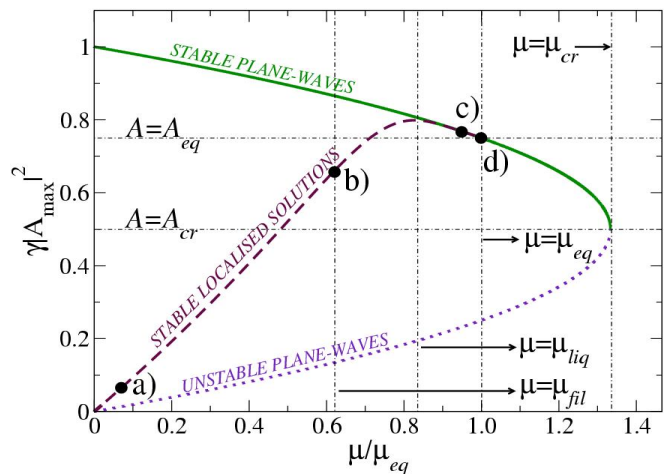


FIG. 1: [Color online] Maximum squared amplitude of different types of stationary solutions of Eq. (1). The continuous and dotted curves correspond to plane waves. The dashed line represents numerically calculated localized eigenstates. The continuous and dashed curves join at  $\gamma|A_{max}|^2 = 0.75$ ,  $|\mu| = |\mu_{eq}|$ . Horizontal lines indicate the critical values  $\gamma|A_{max}|^2 = 0.5$  and  $\gamma|A_{max}|^2 = 0.75$ . Labeled points correspond to solitons that are considered as special examples in the text.

ist with plane waves solutions of constant amplitude  $\Psi_A(x, y, \eta) = Ae^{-i\mu\eta}$ , which lead by substitution in Eq.(1) to  $\mu = \delta|A|^4 - \gamma|A|^2$ . In Fig.1 we have plotted the maximum value of  $\gamma|\Psi|^2$  vs.  $\mu$  in units of  $\mu_{eq}$  for different kinds of stationary solutions of Eq. (1). The continuous and dotted lines correspond respectively to stable and modulationally unstable plane waves[29], whereas the dashed line stands for numerically calculated localized eigenstates[25]. It is known[16] that the shape of the solitons (see dashed profiles in Fig.2) vary from quasi-gaussian shapes for low powers to almost square profiles for beam amplitudes close to a certain critical value of  $\mu = \mu_{eq}$ [16, 25]. At this point the size of the solutions tends to infinity whereas the amplitude of the beam stabilizes at  $|A_{max}|^2 = |A_{eq}|^2 = 0.75\gamma/\delta$ . We will now clarify the reasons of this behavior by using a thermodynamic model.

## III. THERMODYNAMIC MODEL

The appropriate tool to study the equilibrium condition as a function of the number of particles  $N = \int |\Psi|^2 dx dy$  is Landau's grand potential

$$\begin{aligned} \Omega &= H - \mu N = \\ &= \int dx dy \left[ |\nabla_{\perp} \Psi|^2 - \frac{\gamma}{2} |\Psi|^4 + \frac{\delta}{3} |\Psi|^6 - \mu |\Psi|^2 \right], \end{aligned} \quad (2)$$

where the Lagrange multiplier  $\mu$  is the chemical potential for a BEC or the propagation constant in the case of an optical system. For our two-dimensional model the

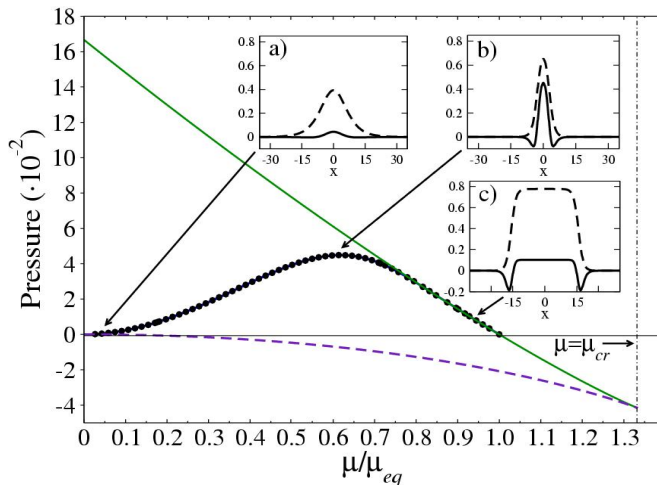


FIG. 2: [Color online] Pressure plots of the plane wave solution branches of Fig.1 (green solid, stable; purple dashed, unstable) and pressure at the center ( $x = 0$ ) of the eigenstates (thick dotted line) corresponding to different points in the dashed line of Fig. 1. Insets: Profiles of the eigenstates (dashed) and pressure distribution (solid). The x-axis indicates the transverse size of the numerically calculated pressure distributions of different eigenstates of eq.(1). We have multiplied both  $\gamma|\Psi|^2$  and  $p$  by 10 and 100 respectively in a) and  $p$  by 10 elsewhere.

area is  $\mathcal{S}$  and we have that  $p = -\partial\Omega/\partial\mathcal{S}$  is the pressure. The equilibrium configurations are obtained when  $\Omega$  is minimized. In particular  $\partial\Omega/\partial\mathcal{S} = 0$  implies that the pressure has to be zero, which for the plane waves of Fig.1 yields  $\partial\Omega/\partial\mathcal{S} = -\frac{\gamma}{2}|A|^4 + \frac{\delta}{3}|A|^6 - \mu|A|^2 = 0$ . There are two possibilities: the trivial case  $|A_{eq}| = 0$  and a uniform phase, with  $\mu_{eq} = -\frac{3\gamma^2}{16\delta}$  and  $|A_{eq}|^2 = 0.75\gamma/\delta$ . In the language of field theory, these solutions are the two possible "vacuum" states of the system. As it can be seen in Fig. 1 the two vacua can be "connected" by the soliton solutions of the dashed line in Fig. 1, which constitute the *instantons* of the theory[26]. It is interesting to notice that the non-zero vacuum solution implies a spontaneously symmetry breaking of the global phase symmetry, which is preserved in the case with  $|A| = 0$ .

This result about the pressure has already been discussed by authors in ref [14] within the framework of the Madelung Transformation (MT), which allows one to establish a formal analogy between nonlinear optics and classical fluid dynamics[27]. With the aid of the MT, an analytical expression for the effective pressure has been derived[14]. Very remarkably, this effective pressure, which is an approximation since it does not take into account the *quantum-mechanical pressure term*[27], calculated for the plane-wave solutions of the CQ-NLSE has the same mathematical expression as the one shown before. Unlike the previous works related in the references, we have calculated the effective pressure by means of the potential given by eq.(2) which contains all the relevant information about the nonlinear system which

is currently being studied.

While the analysis of the infinite plane-wave solutions has already been considered in the literature [14], our discussion of the pressure also applies to the localised soliton solutions, being a central contribution of the present work. We also find a significant difference between the low-power quasi-gaussian solutions and the high-power top-flat solutions of Eq.(1). The expression for plane-waves and top-flat eigenstates can be approximated by the same "reduced" expression for  $p$  given by both the MT and the omega density calculation. In fact, we have shown in Fig.1 that the two branches of solutions, i.e. the localised solitons and the stable plane waves, merge as  $\mu$  approaches  $\mu_{eq}$ , having a radius increasing to infinity, thus in this case it is justified to neglect  $|\nabla_{\perp}\Psi|^2$  in Eq.(2). On the other hand, for the quasi-gaussian eigenstates the previous gradient term is not negligible. In this case, we should calculate  $p$  numerically in the lack of analytical solutions.

The analysis of the pressure can be refined calculating numerically its distribution for different eigenstates as it is plotted in Fig.2. The pressure of the plane wave branches in Fig.1 is plotted as a function of  $\mu/\mu_{eq}$ . Very remarkable is the fact that the pressure of the stable branch is higher than its counterpart of the modulationally unstable solutions branch. In Fig.2 it is also plotted the curve of the eigenstates central pressure. As it can be seen in the graph, the curve corresponding to the eigenstates is bounded by the two curves of the plane-waves branches, so that the existence domain of the filaments phase is limited by them.

In the insets of Fig.2, we show the shape profiles of the eigenstates (dashed line) superposed with their effective pressure profiles (solid lines) which have been conveniently rescaled to fit in the graph. As it can be appreciated in inset a), solitons with  $|\mu| \ll |\mu_{eq}|$  have smooth pressure distributions with a central maximum located at the centroid of the soliton and two negative-valued minima. As the value of  $|\mu|$  increases, the soliton profiles and their corresponding shapes of  $p$  narrow, reaching a minimum width at  $\mu/\mu_{eq} = 0.5$ , which corresponds to a filament soliton solution with the same peak amplitude as the "critical" plane wave with  $|A| = |A_{cr}|$ . This plane-wave marks the border between stable and modulationally unstable plane waves[14]. When the chemical potential reaches the value  $|\mu| = |\mu_{fil}|$  (see inset b), the absolute maximum of  $p$  for eigenstates is obtained, i.e. this filament has the minimum of  $d\Omega/d\mathcal{S}$  at its centroid. We also consider that close to  $|\mu| = |\mu_{liq}|$ , the liquid top-flat eigenstates begin to exist[10]. In fact, the curve of stable localised solutions in Fig.1 has a maximum in that region and both localised solution and stable plane-waves branches seem to merge there. For  $|\mu_{liq}| < |\mu| < |\mu_{eq}|$ , the pressure maximum is located in a flat region (see inset c), tending to zero as  $|\mu|$  approaches the critical value  $|\mu_{eq}|$ , point d) in Fig.1, over which no localized solutions



exist[16].

#### IV. CONDENSATION IN THE PRESENCE OF LINEAR GAIN AND NONLINEAR LOSSES

In this section, we will provide a set of numerical simulations showing the condensation process, i.e., the phase transition from the gaseous phase to an homogeneous coherent “liquid” plane wave solution corresponding to the upper branch in Fig.1. In order to achieve this result, we will perturb an unstable plane wave, corresponding to the lower branch in Fig 1, with a randomly varying noise. This will produce a filamented phase, made of coherent structures whose shape remains qualitatively unchanged, up to smaller scale fluctuations[23].

In order to achieve the non-quantum liquefaction we have included both a linear incoherent pumping mechanism and nonlinear three-body losses[31]. In other words, we have considered  $\delta = \delta^R + i\delta^I$  and we have introduced a linear gain term  $i\Gamma\Psi$  in eq.(1). This corresponds to a continuous load of particles in the system. Note that in this way, we are describing a more realistic non-conservative version of eq.(1), which models an experimentally achievable scenario in the framework of current BEC experiments. In fact, in condensed matter systems it is possible to control the load of particles and two and three-body recombination within the coherent atomic cloud[20].

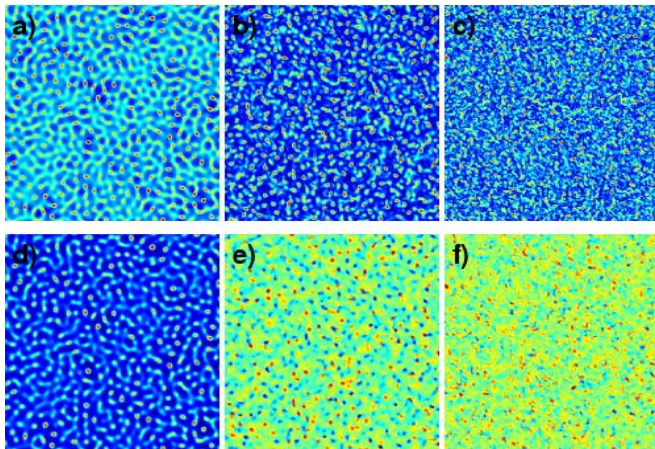


FIG. 3: [Color online] Numerical simulation of the evolution of a set of filaments in presence of linear gain and three-body losses. Propagation algorithm parameters:  $\gamma = 1$ ,  $\Gamma = 10^{-4}$ ,  $\delta = 1 + 0.1i$ . Top: pseudocolor maps of the amplitude. Bottom: pseudocolor maps of the phase corresponding to the amplitudes above. As it can be appreciated in the sequence of snapshots, the initial condition which has a certain level of organization, evolves towards a complete disordered situation, i.e., the diluted disordered gaseous phase arises. The frames correspond to values of the adimensional variable  $\eta$ : 0 (a, d), 1000 (b, e) and 4000 (c, f).

On the other hand, in nonlinear optics, this kind of nonlinear models are well-known in the frame of complex

Ginzburg-Landau (G-L) equations used to describe wide-aperture laser cavities[33]. Although it is always possible to control the linear gain introduced in the system, three-body losses are often imposed by the nonlinear response of the material, so it is not possible to manage the dissipation terms of the system. However, by means of electromagnetic induced transparency techniques, it is possible to customize the nonlinear optical response of cold atomic ensembles like Rb[11] so that the nonlinear refractive index corresponds to the one given by the modified eq.(1) analyzed in the current section of the paper. Therefore our model, and its predicted phenomenon of liquefaction that we will demonstrate below, can correspond both to realistic BEC and nonlinear optical systems.

In Fig.3, the initial state consists of an incoherent set of filaments with a randomly varying phase distribution. Within this apparent disorder, some coherent uncorrelated structures (filaments) exist and can be observed in Fig.3 a). In this simulation, we have considered a nonlinear parameter regime where the linear gain was not enough to compensate the three-body dissipative term. As a consequence, certain degree of coherence is lost since the filaments disappear and only the noisy background is observed, as shown by snapshot c) in Fig.3). Starting

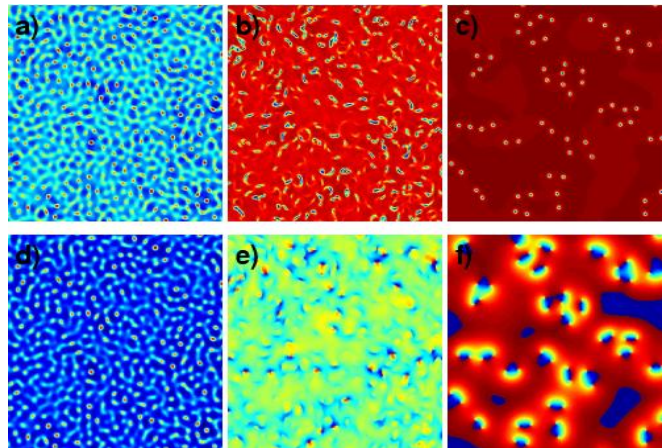


FIG. 4: [Color online] Same as in Fig.3, but with a modified value of the linear gain  $\Gamma = 8 \cdot 10^{-4}$ . Other parameters as in Fig.3. In this simulation, the final state is a homogeneous background of coherent liquid with amplitude  $|A| = |A_{eq}|$ , but it is remarkable that the wavefront presents some topological defects (vortices) which distort the phase distribution of the resulting liquid plane wave as it can be observed in the phase maps on the bottom row. The frames correspond to values of the adimensional variable  $\eta$ : 0 (a, d), 1000 (b, e) and 4000 (c, f).

from the same initial condition but increasing the linear gain term over a certain threshold, we have performed the simulation shown in Fig.4. In this case, we see that the system evolves towards an homogeneous plane wave by the combined effect of adding particles to the initial random state and dissipation due to many-body inelastic processes. This relaxation process is well-known in the

context of the complex G-L equations and is attributed to the non-conservative nature of the model[32]. Nevertheless, as our theory predicts, the system will tend to form a particular plane wave of the stable “liquid” upper branch of Fig.1, the one with zero pressure. This illustrates the tendency of the system to reach the non-zero vacuum state with  $|A|^2 = 3\gamma/4\delta$ . Very remarkably, dur-

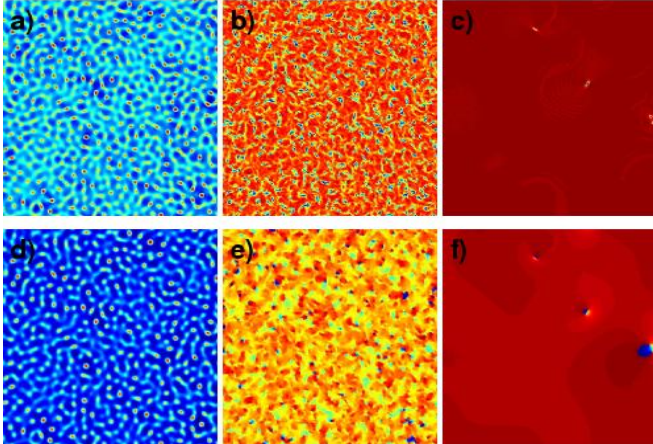


FIG. 5: [Color online] Numerical simulation of the evolution of a set of filaments in presence of C-Q nonlinear gain and loss. The linear gain term used in the previous simulations has been replaced here by a nonlinear gain term  $i\chi|\Psi|^2$ , where  $\chi = 0.1$ . Other parameters are:  $\gamma = 1$ ,  $\delta = 1 + 0.1i$ . Top: pseudocolor maps of the amplitude. Bottom: pseudocolor maps of the phase corresponding to the amplitudes above. Qualitatively, the same results of Fig.4 are obtained. However, it is important to note that in this case, the robust topological structures with nonzero vorticity which appear during the dynamical liquefaction process are annihilated, resulting in a final homogeneous background with amplitude  $|A| = |A_{eq}|$  and constant phase distribution, as it can be seen in snapshot f). The frames correspond to values of the dimensional variable  $\eta$ : 0 (a, d), 1000 (b, e) and 4000 (c, f).

ing the process pairs of vortex-antivortex with topological charges  $m_v = 1, m_{av} = -1$  are formed (see bottom phase maps in Fig.4), so that the constant phase of the

emerging coherent wave remains hidden by the overlapping of the different vortex rotating phase-distributions. Vortices are very robust topological structures[12] and in our simulations they remain stable as far as we could follow the numerical simulations.

Finally, we have considered the effect of replacing the linear gain term by a nonlinear gain term of the form  $i\chi|\Psi|^2$ . In this situation, the numerical results are qualitatively the same as in Fig.4, although it can be observed that in the last stage of the evolution the vortices are annihilated. In snapshot f) of Fig.4, it can be seen how the underlying plane wave, which emerges after the dynamical process as described above, has a homogeneous phase distribution. We think that this result is a very interesting example of a self-organization process, where coherence is produced from disorder, with evident practical applications.

## V. CONCLUSIONS

We have shown in the present work that a system of  $N$  equal bosons in a system with competing nonlinearities can undergo a phase transition from a gas to a liquid state. The process takes place at zero temperature without any quantum effect and it is only ruled by nonlinear interactions. Finally, we have shown that a cubic-quintic medium with complex susceptibilities exhibiting linear gain and nonlinear losses, will tend to produce a homogeneous phase liquid distribution starting from a collection of non-correlated filaments. This opens the door for experiments in the field of BEC systems in ultracold gases.

## VI. ACKNOWLEDGMENTS

H. M. thanks A. J. Leggett and A. Ferrando for useful discussions and Y. Castin, J. Ho and G. V. Shlyapnikov for warm hospitality at Inst. Henri Poincaré. This work was supported by MEC, Spain (projects FIS2006-04190 and FIS2007-62560) Xunta de Galicia (project PGIDIT04TIC383001PR and D.N. grant from Consellería de Educación, Xunta de Galicia).

- 
- [1] A.J. Leggett, “*Quantum Liquids: Bose Condensation and Cooper Pairing in Condensed-Matter Systems*”, (Oxford University Press, N.Y. 2006).
  - [2] C. Sulem and P.L. Sulem, “*Nonlinear Schrödinger Equations: Self-Focusing and Wave Collapse*”, (Springer-Verlag, N.Y. 1999).
  - [3] M. D. Miller, L. H. Nosanow, and L. J. Parish, Phys. Rev. B **15**, 214-229 (1977).
  - [4] R. Y. Chiao, Opt. Commun. **179**, 157–166 (2000).
  - [5] C. Connaughton *et al.*, Phys. Rev. Lett. **95**, 263901 (2005).
  - [6] A. D. Greentree, *et al.*, Nature Phys., **2**, 856-861 (2006).
  - [7] S. Sadchev, Science **288**, 475-479 (2000).
  - [8] S. L. Sondhi, *et al.*, Rev. Mod. Phys. **69**, 315-333 (1997).
  - [9] E. L. Bolda, R. Y. Chiao and W. H. Zurek, Phys. Rev. Lett. **86**, 416–419 (2001); R. Y. Chiao *et al.*, J. Phys. B: At. Mol. Opt. Phys **37**, S81–S89 (2004); R. Y. Chiao *et al.*, Phys. Rev. A **69**, 063816 (2004); A. Tanzini and S.P. Sorella Phys. Lett. A **263**, 43–47 (1999).
  - [10] H. Michinel *et al.*, Phys. Rev. E **65**, 066604 (2002).
  - [11] H. Michinel, M. J. Paz-Alonso and V. M. Pérez García, Phys. Rev. Lett. **96**, 023903 (2006).
  - [12] M. J. Paz-Alonso *et al.*, Phys. Rev. E **69**, 056601 (2004).
  - [13] A. H. Piekara, J. S. Moore, and M. S. Feld, Phys. Rev. A **9**, 1403–1407 (1974).
  - [14] C. Josserand, Y. Pomeau and S. Rica, Phys. Rev. Lett. **75**, 3150–3153 (1995); C. Josserand, Phys. Rev. E **60**, 482–491 (1999);

- [15] C. Josserand and Sergio Rica, Phys. Rev. Lett. **78**, 1215–1218 (1997).
- [16] M. Quiroga-Teixeiro and H. Michinel, J. Opt. Soc. Am. B **14**, 2004–2009 (1997); D. Mihalache, *et al.*, Phys. Rev. Lett. **88**, 073902 (2002).
- [17] H. Michinel, J. Campo-Táboas, M. L. Quiroga-Teixeiro, J. R. Salgueiro, and R. García Fernández, J. Opt. B: Quantum Semiclass. Opt. **3**, 314 (2001); M. J. Paz-Alonso and H. Michinel, Phys. Rev. Lett. **94**, 093901 (2005).
- [18] D. E. Edmundson and R. H. Enns, Phys. Rev. A **51**, 2491–2498 (1995);
- [19] M. Centurion *et al.*, Phys. Rev. A **71**, 063811 (2005).
- [20] H. P. Buchler, A. Micheli, and P. Zoller, Nature Phys. **3**, 726–731 (2007).
- [21] S. Tzortzakis *et al.*, Phys. Rev. Lett. **86**, 24 (2001); A. Couairon, Phys. Rev. A **68**, 015801 (2003); S. Skupin *et al.*, Phys. Rev. E **70**, 046602 (2004); L. Bergé *et al.*, Phys. Rev. Lett. **92**, 22 (2004); C. Ruiz *et al.*, Phys. Rev. Lett. **95**, 053905 (2005).
- [22] F. Smektala, C. Quemard, V. Couderc, and A. Barthelemy, J. Non-Cryst. Sol., **274**, 232–237 (2000).
- [23] R. Jordan and C. Josserand, Phys. Rev. E **61**, 2 (2000).
- [24] A. Bulgac, Phys. Rev. Lett. **89**, 050402 (2002); A. Gamal *et al.*, Phys. Rev. A **61**, 051602(R) (2000); H.-W. Hammer and D.T. Son, Phys. Rev. Lett. **93**, 250408 (2004).
- [25] H. Michinel, J. R. Salgueiro, and M.J. Paz-Alonso, Phys. Rev. E **70**, 066605 (2004).
- [26] T. Schafer and E. V. Shuryak, Rev. Mod. Phys. **70**, 323–425 (1998).
- [27] C. Coste, Eur. Phys. J. B. **1**, 245–253 (1998).
- [28] M. -O. Mewes, M. R. Andrews, D. M. Kurn, D. S. Durfee, C. G. Townsend and W. Ketterle, Phys. Rev. Lett. **78**, 582 (1997).
- [29] V. I. Bespalov and V. I. Talanov, JETP Lett. **3**, 307 (1966).
- [30] M. Centurion, *et al.*, Phys. Rev. A **74**, 069902(E) (2006).
- [31] E. Braaten and H.W. Hammer, Phys. Rev. Lett. **87**, 16 (2001).
- [32] LC. Crasovan, BA. Malomed and D. Mihalache, Phys. Rev. E **63**, 016605 (2001); P. Grelu, J. Soto-Crespo and N. Akhmediev, Opt. Express **13**, 23, pp: 9352–9360 (2005) S. Mancas, SR. Choudhury, Chaos, Solitons and Fractals, **27**, 5, pp: 1256–1271 (2006)
- [33] J.M. Soto-Crespo, P. Grelu, and N. Akhmediev, Opt. Express **14**, 4013–4025 (2006).